Mean scalar concentration profile in a sheared and thermally stratified atmospheric surface layer

Gabriel G. Katul, Dan Li, Marcelo Chamecki, and Elie Bou-Zeid

Phys. Rev. E **87**, 023004 — Published 13 February 2013

DOI: 10.1103/PhysRevE.87.023004

Mean scalar concentration profile in a sheared and thermally stratified atmospheric surface layer

Gabriel G. Katul,[1,2] Dan Li,[3] Marcelo Chameki,[4] and Elie Bou-Zeid[3]

[1]*Nicholas School of the Environment, Duke University, Durham, NC 27708-0328, USA*
[2]*Department of Civil and Environmental Engineering, Duke University, Durham, NC 27708*
[3]*Department of Civil and Environmental Engineering, Princeton University, Princeton, NJ 08544, USA*
[4]*Department of Meteorology, The Pennsylvania State University, University Park, PA 16802, USA*

Using only dimensional considerations, Monin and Obukhov proposed a 'universal' stability correction function $\phi_c(\zeta)$ that accounts for distortions caused by thermal stratification to the mean scalar concentration profile in the atmospheric surface layer when the flow is stationary, planar homogeneous, fully turbulent, and lacking any subsidence. For nearly six decades, their analysis provided the basic framework for almost all operational models and data interpretation in the lower atmosphere. However, the canonical shape of $\phi_c(\zeta)$ and the departure from the Reynold's analogy continue to defy theoretical explanation. Here, the basic processes governing the scalar-velocity co-spectrum, including buoyancy and the scaling laws describing the velocity and temperature spectra, are considered via a simplified co-spectral budget. The solution to this co-spectral budget is then used to derive $\phi_c(\zeta)$, thereby establishing a link between the energetics of turbulent velocity and scalar concentration fluctuations and the bulk flow describing the mean scalar concentration profile. The resulting theory explains all the canonical features of $\phi_c(\zeta)$, including the onset of power-laws for various stability regimes and their concomitant exponents, as well as the causes of departure from Reynold's analogy.

I. INTRODUCTION

The exchange of heat, water vapor, ozone, carbon dioxide and other greenhouse gases between the land or ocean and the lower atmosphere is complicated by the co-existence of shear- and buoyancy-generated (or dissipated) turbulence. Monin and Obukhov Similarity Theory [1, 2], hereafter referred to as MOST, describes how thermal stratification distorts the mean scalar concentration (C) profile in the so-called atmospheric surface layer using only dimensional analysis. The atmospheric surface layer is a region whose lower bound is much larger than the height of the roughness elements at the ground surface and whose upper bound is not too high up in the atmosphere to be impacted by Coriolis effects. Thus, the atmospheric surface layer region encompasses much of the human and biological processes. Despite some six decades after its inception, MOST remains the basic 'work-horse' employed when coupling land or oceanic fluxes to the atmospheric state in virtually all climate, oceanic, regional atmospheric, hydrological and ecological models [3]. MOST introduces a dimensionless stability parameter ζ that measures the height at which mechanical production of turbulent kinetic energy balances the buoyancy production (or destruction). Distortions produced by thermal stratification to the otherwise logarithmic mean scalar concentration profile can then be encoded in a so-called 'universal' stability correction function $\phi_c(\zeta)$, which so far has been empirically determined from experiments [5]. The shape and universal character of $\phi_c(\zeta)$ have been documented across several field experiments for heat, and other scalars (e.g. water vapor), and embody a large corpus of data on scalar exchange in the atmospheric surface layer as evidenced by Figure 1. Yet, despite their wide-spread usage, the canonical form of these scalar stability correction functions continue to defy theory, even for the most idealized flow conditions. The aim of this work is to present a co-spectral theory that predicts the canonical shape of $\phi_c(\zeta)$, and by extension, the scalar eddy-diffusivity for such idealized flow conditions. The theory provides an analytical link between $\phi_c(\zeta)$ and the basic turbulent processes governing scalar transport that result in the universal character of $\phi_c(\zeta)$. It also establishes the organizing framework for diagnosing why several field experiments report anomalous $\phi_c(\zeta)$ over oceans and land [10, 11].

II. THEORY

As earlier noted, MOST is restricted to idealized incompressible atmospheric surface layer flows associated with a number of simplifications to the Reynolds-averaged longitudinal momentum balance and scalar continuity equations given by

$$\frac{\partial U}{\partial t} + U_j \frac{\partial U}{\partial x_j} = \nu \frac{\partial^2 U}{\partial x_j \partial x_j} - \frac{\partial \overline{u' u'_j}}{\partial x_j} - \frac{1}{\rho}\frac{\partial P}{\partial x}, \tag{1}$$

$$\frac{\partial C}{\partial t} + U_j \frac{\partial C}{\partial x_j} = D_m \frac{\partial^2 C}{\partial x_j \partial x_j} - \frac{\partial \overline{u'_j c'}}{\partial x_j}, \tag{2}$$

where t is time, $x_j = (x, y, z)$ represents the longitudinal ($= x$), lateral ($= y$), and vertical ($= z$) directions, respectively. The longitudinal direction is aligned along the mean wind direction so that the mean lateral velocity is zero. The U, C, and P represent the Reynolds-averaged longitudinal velocity, scalar concentration, and

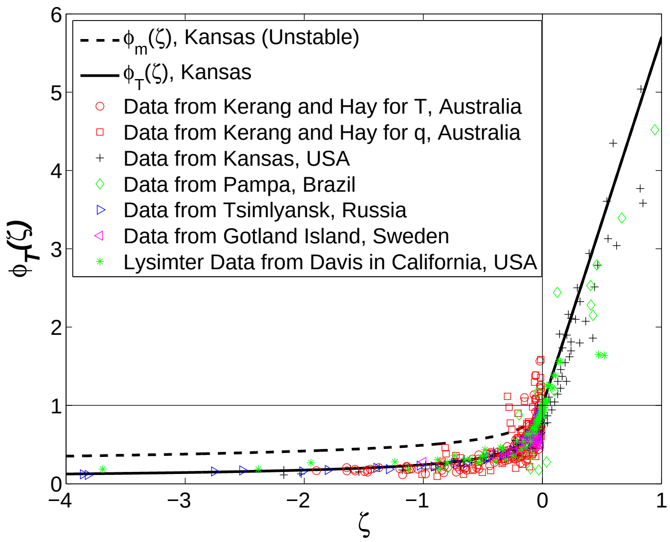

FIG. 1. (Color on-line): The universal shape of $\phi_c(\zeta)$ for air temperature determined from the Kansas experiment in the atmospheric surface layer (lines). Note the linear increase of $\phi_c(\zeta)$ with increasing ζ for stable atmospheric conditions ($\zeta > 0$) and the power-law decline in $\phi_c(\zeta)$ with increasing $-\zeta$ for unstable atmospheric conditions ($\zeta < 0$). The so-called Businger-Dyer (BD) stability correction functions for $\phi_m(\zeta)$ and $\phi_c(\zeta)$, inferred from the Kansas experiment, are shown as lines. For stable conditions, $\phi_c(\zeta)$=$\phi_m(\zeta)$, where such equality between the momentum ($\phi_m(\zeta)$) and scalar ($\phi_c(\zeta)$) stability correction functions is often referred to as Reynolds analogy. For unstable conditions, $\phi_c(\zeta)$=$\phi_m(\zeta)^2$, a signature of a break-down of Reynold's analogy. Other experiments on air temperature (C=T) and water vapor (C=q) exchange from different geographic regions around the world are also presented for illustration (as symbols). These experiments include the influential Kansas data [4], the data collected in the towns of Kerang and Hay [5] on heat and water vapor exchange in Australia, the data on heat exchange over the Pampas in Brazil [6], the long-term (day-time only) heat exchange data from the Steppe region in Russia [7], the long-term data on heat exchange from the island of Gotland in the Baltic Sea [8], data for water vapor exchange using drag plate (to estimate u_*) and weighing lysimeter (to estimate water vapor fluxes) from University of California Davis, California, USA [9].

pressure, respectively, ρ is the mean air density, ν is the air kinematic viscosity, D_m is the molecular diffusivity of scalar C in air, $u_i' = (u', v', w')$ are the component-wise turbulent velocity excursions in direction x_i, c' is the turbulent scalar concentration fluctuation, and unless otherwise stated, primed quantities represent turbulent excursions from the Reynolds-averaged mean state represented by overbar or capital letter symbols. Hence, the instantaneous velocity and concentration can be expressed as $u_i = U_i + u_i'$ and $c = C + c'$. As discussed elsewhere [2], the proper averaging operator that must be employed on these equations is ensemble averaging; however, measurements in the atmospheric surface layer are routinely presented as time averages. Given the near impossibility of repeating experiments for identical meteorological states in natural conditions to compute ensemble averages, it is customary to assume atmospheric surface layer flows are ergodic so that ensemble averaging and time averaging converge. It is for this reason that time averaging periods used in atmospheric surface layer studies are on the order of 1 hour so as to ensure that a single period includes an ensemble of eddies (usually characterized by time scales of tens of seconds) collected under similar meteorological conditions. Hereafter, the term Reynolds averaging is used to indicate both time averaging when interpreting field measurements, or ensemble averaging when interpreting equations as is conventional in atmospheric turbulence studies.

MOST assumes that the flow is (i) characterized by high Reynolds and Peclet numbers (i.e. neglect molecular viscosity and diffusivity relative to their turbulent counterparts), (ii) stationary (i.e. $\partial(.)/\partial t = 0$) and planar-homogeneous (i.e. $\partial(.)/\partial x = \partial(.)/\partial y = 0$), and (iii) lacking any subsidence (i.e. $U_3 = W = 0$) and mean horizontal pressure gradient (i.e. $\partial P/\partial x = 0$). For these idealized states, the mean longitudinal momentum balance and the mean scalar budget reduce to $\partial\overline{w'u'}/\partial z = 0$ and $\partial\overline{w'c'}/\partial z = 0$. Hence, the turbulent stresses (i.e. $\overline{w'u'}$) and scalar fluxes (i.e. $\overline{w'c'}$) do not vary with z. It is for this reason that the atmospheric surface layer subjected to MOST assumptions is often labeled as the constant-stress or constant-flux layer [5].

A. Background and Definitions

The stability correction functions for momentum $\phi_m(\zeta)$ and for an arbitrary scalar $\phi_c(\zeta)$ in the atmospheric surface layer are defined as

$$\phi_m(\zeta) = \frac{-k_v u_* z}{\overline{w'u'}} \frac{\partial U(z)}{\partial z} = \frac{-k_v u_* z}{\frac{1}{S(z)} \int\limits_0^\infty F_{wu}(z, K) dK}, \quad (3)$$

$$\phi_c(\zeta) = \frac{-k_v u_* z}{\overline{w'c'}} \frac{\partial C(z)}{\partial z} = \frac{-k_v u_* z}{\frac{1}{\Gamma(z)} \int\limits_0^\infty F_{wc}(z, K) dK}, \quad (4)$$

where $\overline{w'u'} = -u_*^2$, u_* is the friction velocity and does not vary with z, $S(z) = \partial U(z)/\partial z$ is the mean velocity gradient, $\Gamma(z) = \partial C(z)/\partial z$ is the mean scalar concentration gradient, $k_v \approx 0.4$ is the von Karman constant, $\zeta = z/L$ where $L = -u_*^3/(k_v \beta \overline{w'T'})$ is the Obukhov length [1, 12, 13], $\beta = g/T_a$, g is the gravitational acceleration, T_a is the absolute mean air temperature, $\overline{w'T'}$ is the sensible heat flux, and $F_{wc}(z, K)$ and $F_{wu}(z, K)$ are the scalar flux and momentum flux co-spectra for wavenumber K at a given height z. In principle, F_{wu} and F_{wc} should be integrated over the surface of a sphere of radius K, where K is the scalar wavenumber. However, because co-spectra reported in conventional atmospheric surface layer studies are calculated from single point measurements [14] and then converted to streamwise one-dimensional cuts using Taylor's frozen turbulence hypothesis [15, 16], one-dimensional co-spectra (and spectra) are used here and K can be interpreted as the wavenumber in the streamwise direction. The co-spectra are height-dependent; however, upon integrating them across all the wavenumber range, they become independent of z and given by $\overline{w'u'}$ and $\overline{w'c'}$ (both fluxes are height independent as previously shown). A specific illustration of this height independence of the integrated co-spectra is discussed later. The atmospheric surface layer flow is referred to as unstable when $\zeta < 0$ (e.g. when the surface heats up during the day so that $\overline{w'T'} > 0$) and stable when $\zeta > 0$ (e.g. when the surface cools during nighttime so that $\overline{w'T'} < 0$). These definitions for $\phi_m(\zeta)$ and $\phi_c(\zeta)$ imply that the turbulent diffusivities for momentum and scalars are $K_{tm} = k_v u_* z/\phi_m(\zeta)$ and $K_{tc} = k_v u_* z/\phi_c(\zeta)$.

In the inertial subrange, a range delineated by eddy sizes much smaller than the integral length scale of the flow but much larger than the Kolmogorov viscous dissipation length scale [17, 18], the co-spectra $F_{wu}(z,K)$ and $F_{wc}(z,K)$ are classically given by [14, 19]

$$F_{wu}(z,K) = C_{wu} S(z)\, \varepsilon(z)^{1/3} K^{-7/3}, \tag{5}$$

$$F_{wc}(z,K) = C_{wc} \Gamma(z)\, \varepsilon(z)^{1/3} K^{-7/3}, \tag{6}$$

where $\varepsilon(z)$ is the mean turbulent kinetic energy dissipation rate, and C_{wu} and C_{wc} are similarity constants (discussed later). Because the flow in the inertial subrange is locally homogeneous and isotropic, the scalar wavenumber K can be reasonably approximated by its one-dimensional longitudinal cut as earlier noted. A number of studies have also shown that inertial subrange scaling laws are not sensitive to the local isotropy assumption [20]. Stated differently, inertial subrange scaling laws extend over a much broader range of K values within the inertial subrange when compared to the range of K values inferred from locally-isotropic predictions of velocity components' spectral ratios. If the turbulent flow field is energetically near its equilibrium state with the production and destruction of turbulent kinetic energy in balance, the turbulent kinetic energy budget equation results in

$$\varepsilon(z) = \frac{u_*^3}{k_v z} \left(\phi_m(\zeta) - \zeta\right). \tag{7}$$

When the integrated effects of all eddies much larger than z do not significantly contribute to the co-spectra $F_{wu}(z,K)$ and $F_{wc}(z,K)$ (this issue will also be revisited later), then it follows that $-\overline{w'u'} = \int_{1/z}^{\infty} F_{wu}(z,K) dK$ and $\overline{w'c'} = \int_{1/z}^{\infty} F_{wc}(z,K) dK$. As earlier noted, the co-spectral expressions explicitly contain z; however, upon integration with respect to K, the z cancels and the constant stress and constant flux assumptions are preserved provided z is treated independent of K in the integration with respect to K. To illustrate, consider the near-neutral condition with $\varepsilon(z) = u_*^3/(k_v z)$ and $S(z) = u_*/(k_v z)$, where upon integrating $F_{wu}(z,K)$ given by equation 5 within the prescribed limits, the expected $-\overline{w'u'} = u_*^2$ is recovered when $C_{wu} = (4/3) k_v^{(4/3)}$. Similar arguments can be made for $\overline{w'c'}$, the integrated $F_{wc}(z,K)$ and their z independence.

For any stability condition, direct links between the co-spectra and the stability correction functions can now be established via

$$\phi_m(\zeta) \approx \frac{-k_v u_* z}{\frac{1}{S(z)} \int_{1/z}^{\infty} F_{wu}(z,K) dK} \approx \frac{1}{\left(\phi_m(\zeta) - \zeta\right)^{1/3}}, \tag{8}$$

$$\phi_c(\zeta) \approx \frac{-k_v u_* z}{\frac{1}{\Gamma(z)} \int_{1/z}^{\infty} F_{wc}(z,K) dK} \approx \frac{1}{\left(\phi_m(\zeta) - \zeta\right)^{1/3}}. \tag{9}$$

The constants C_{wu} and C_{wc} should be selected to ensure that $\phi_m(0) = 1$ and $\phi_c(0) = 1$. This constraint on ϕ_c is repeatedly used here so that many combinations of similarity or integration constants equate to unity making the final outcome insensitive to the precise values of these constants. The equations 8 and 9 can be re-written as two OKEYPS (after Obukhov, Kazansky, Ellison, Yamamoto, Panofsky, and Sellers) equations [21–23],

$$\left(\phi_m(\zeta)\right)^3 \left(\phi_m(\zeta) - \zeta\right) = 1, \tag{10}$$

$$\left(\phi_c(\zeta)\right)^3 \left(\phi_m(\zeta) - \zeta\right) = 1. \tag{11}$$

An obvious solution to the scalar OKEYPS equation is the Reynolds analogy, with $\phi_c(\zeta) = \phi_m(\zeta)$. According to Large Eddy Simulations [24] and many field experiments [3, 25–27], $\phi_m(\zeta) = (1 - 16\zeta)^{-1/4}$ when $\zeta < 0$ and $\phi_m(\zeta) = (1 + 4.7\zeta)$ when $\zeta > 0$. A derivation of these $\phi_m(\zeta)$ functions and their links to the energy spectrum is presented elsewhere [28] and is not repeated here. The $\phi_c(\zeta) = \phi_m(\zeta)$ solution is supported by several experiments for stable atmospheric conditions as evidenced from Figure 1, but not for unstable conditions [15].

A refinement to the previous argument is that eddies that vertically transport scalars may be larger or smaller than z depending on ζ. In general, with increased surface heating, eddies that contribute to vertical scalar fluxes are larger than z, and conversely, for stable atmospheric conditions. Let $\Lambda_u(\zeta)/\Lambda_u(0) = f_{wu}(\zeta)$ and $\Lambda_c(\zeta)/\Lambda_c(0) = f_{wc}(\zeta)$ be the ratios of largest eddy sizes that appreciably contribute to $F_{wu}(K)$ and $F_{wc}(K)$ under some stability ζ normalized by the value under neutral stability. Let $\Lambda_u(0) = s_u z$ and $\Lambda_c(0) = s_c z$ be the neutral reference scales of the dominant eddies, which are allowed to be proportional rather than strictly equal to z, where s_u and s_c are now proportionality constants that do not vary with atmospheric stability. Hence, $f_{wc}(\zeta)$ and $f_{wu}(\zeta)$ represent relative departures in eddy sizes from their neutral state due to thermal stratification (i.e. $f_{wc}(0) = f_{wu}(0) = 1$). Replacing the $1/z$ integration limit in equations 8 and 9 by $1/(s_u f_{wu}(\zeta) z)$ and $1/(s_c f_{wc}(\zeta) z)$, it follows that

$$\phi_m(\zeta)^3 \left(\phi_m(\zeta) - \zeta\right) \approx \frac{1}{\left(s_u f_{wu}(\zeta)\right)^4}, \tag{12}$$

$$\phi_c(\zeta)^3 \left(\phi_m(\zeta) - \zeta\right) \approx \frac{1}{\left(s_c f_{wc}(\zeta)\right)^4}. \tag{13}$$

Hereafter, the lower integral limit in equations 8 and 9 is replaced by $1/(s_c f_{wc}(\zeta) z)$ unless otherwise stated. With the two equations above, the turbulent Prandtl number (Pr) is reduced to

$$\mathrm{Pr} = \frac{K_{tm}}{K_{tc}} = \frac{\phi_c(\zeta)}{\phi_m(\zeta)} = \left(\frac{s_u f_{wu}(\zeta)}{s_c f_{wc}(\zeta)}\right)^{4/3}. \tag{14}$$

Field experiments have shown that $s_u = s_c \approx 1$ and that $f_{wc}(\zeta) \approx f_{wu}(\zeta)$ for both stable and unstable conditions [6, 15]. $f_{wc}(\zeta)^{-1}$ varies linearly with ζ for stable conditions ($f_{wc}(\zeta)^{-1} = (1 + \alpha\zeta)$, with the constant $\alpha \approx 1.7$ here) and remains unity ($f_{wc}(\zeta) = 1$) for neutral and unstable conditions[6, 14, 15]. The fact that $s_u = s_c \approx 1$ implies that the eddies most important for momentum and scalar transfer under near-neutral conditions are eddies touching the ground or attached eddies [29]. However, this derivation still cannot explain why Pr is different from unity (i.e. why the Reynolds analogy fails) and varies with atmospheric stability for unstable conditions ($\zeta < 0$) as evidenced by the data in Figure 1 that shows $\phi_m(\zeta) > \phi_c(\zeta)$. Alternative mechanisms are needed to unlock the causal difference between $\phi_m(\zeta)$ and $\phi_c(\zeta)$ for unstable conditions. The previous approach assumed that $F_{wu}(z, K)$ and $F_{wc}(z, K)$ follow their inertial subrange scaling from $K \in [1/\Lambda, \infty]$, a result that need not hold for scalars. Several processes regulating the magnitude and shape of $F_{wc}(z, K)$ beyond eddy size adjustment to changes in ζ, not considered in the discussion above, are discussed next. The sequential inclusion of each of these processes in a proposed budget equation describing $F_{wc}(z, K)$, and the concomitant modification to $\phi_c(\zeta)$, is then presented.

B. A simplified co-spectral budget

Because the terms in the co-spectral budget resemble those in the turbulent scalar flux budget, a brief summary of the scalar flux budget in the idealized atmospheric surface layer, given as

$$\frac{\partial \overline{w'c'}}{\partial t} = 0 = -\overline{w'w'}\Gamma(z) - \frac{\partial \overline{w'w'c'}}{\partial z} - \frac{1}{\rho}\overline{c'\frac{\partial p'}{\partial z}} + \frac{g}{T_a}\overline{c'T'} - M_d \tag{15}$$

is first discussed. On the right hand side, the first term represents the scalar flux production due to a finite $\Gamma(z)$, the second represents the vertical flux transport term by turbulence, the third represents the pressure-scalar interaction term whose role is to de-correlate w' and c' and which is thus a net sink in the equation, the fourth is the buoyancy term that can serve as a production or dissipation term depending on the scalar being analyzed, and M_d represents all the molecular destruction terms, often much smaller than their pressure-scalar interaction counterparts for very high Peclet number flows. When the scalar being analyzed is air temperature, the buoyancy term becomes positive and dependent on the temperature variance ($=\overline{T'T'}$), which is the main focus here. However, the derivation is maintained for an arbitrary scalar for completeness. The budget equation for the co-spectrum $F_{wc}(z, K)$, derived elsewhere [30, 31] but expanded here to include the thermal stratification term (i.e. the contributions arising from $(g/T_a)\overline{c'T'}$ in the scalar flux budget), is given by

$$\frac{\partial F_{wc}(z, K)}{\partial t} + (\nu + D_m)K^2 F_{wc}(z, K) = G(z, K), \tag{16}$$

where $G(z, K) = P(z, K) + T_{wc}(z, K) + \pi(z, K) + \beta F_{Tc}(z, K)$, $P(z, K) = \frac{2}{3}\Gamma(z)E(z, K)$ is the production term (analogous to $\overline{w'w'}\Gamma$), $E(z, K)$ is the vertical velocity energy spectrum at z, $T_{wc}(z, K)$ is a non-linear turbulent flux transport term arising from Fourier-transforming the triple correlation function $\overline{(u_i(x)u_3(x + r)c(x) - u_i(x + r)u_3(x + r)c(x))}$ with r being the separation distance between two points, and $\pi(z, K)$ is the pressure-scalar interaction term, $F_{Tc}(z, K)$ is the scalar-temperature co-spectrum. The term $\beta F_{Tc}(z, K)$ arises from the presence of $(g/T_a)\overline{c'T'}$ noted earlier in the Reynolds-averaged scalar flux budget. As discussed elsewhere [30], direct numerical simulations at moderate Reynolds number suggest that the sum of the two molecular terms $|(\nu + D_m)K^2 F_{wc}(K)|$ is less than 10% of $|\pi(K)|$, and their contribution further diminishes with increasing Reynolds number. Hence, for the high Reynolds number flow characterizing the idealized atmospheric surface layer, these two molecular terms are ignored relative to $\pi(K)$ throughout. If a Rotta-like model modified to include buoyancy effects is invoked for the pressure-scalar interaction term [32–34], then

$$\pi(z, K) = -A_\pi \frac{F_{wc}(z, K)}{\tau(z, K)} + \frac{1}{3}\beta F_{Tc}(z, K), \tag{17}$$

where $\tau(z, K) = \varepsilon(z)^{-1/3} K^{-2/3}$ is a wavenumber dependent timescale at height z. The Rotta model has been the subject of numerous studies [35], and despite its limitations, remains widely employed in modeling pressure-scalar interactions in high Reynolds number turbulent flows. The co-spectral nonlinear turbulent flux transport term was shown elsewhere to act mainly to transport covariance away from the peak in the co-spectra [30] (i.e. transports covariance from scales with higher to scales with lower covariance). As such, it may be modeled as

$$T(z,K) = -A_T \frac{\partial}{\partial K}\left(\varepsilon(z)^{1/3}\ K^{5/3} F_{wc}(z,K)\right). \quad (18)$$

Even with all these simplifications, solving for $F_{wc}(z,K)$ requires the energy spectrum $E(z,K)$, the temperature-scalar co-spectrum $F_{Tc}(z,K)$, $\Gamma(z)$, $\varepsilon(z)$, as well as the two closure constants A_π and A_T, discussed next.

C. The Neutral Equilibrium State

In the absence of buoyancy effects ($\beta \approx 0$) and turbulent flux co-spectral transport contributions, the co-spectral budget reduces to a balance between production and pressure-scalar induced de-correlation between w' and c' (equivalent to a dissipation of $\overline{w'c'}$) given as

$$0 = \frac{2}{3}\Gamma(z)E(z,K) - A_\pi \varepsilon(z)^{1/3}\ K^{2/3} F_{wc}(z,K), \quad (19)$$

and results in

$$F_{wc}(z,K) = \frac{2}{3}\frac{1}{A_\pi}\Gamma(z)\varepsilon(z)^{-1/3}\ K^{-2/3} E(z,K). \quad (20)$$

Upon assuming the classical Kolmogorov (hereafter referred to as K41) scaling within the inertial subrange for $E(z,K)$, given as [17, 36]

$$E(z,K) = C_o \varepsilon(z)^{2/3} K^{-5/3}, \quad (21)$$

one obtains $F_{wc}(z,K) = C_{wc}\Gamma(z)\varepsilon(z)^{1/3}\ K^{-7/3}$, where $C_{wc} = C_o(2/3/A_\pi)$, and $C_o = 0.55$ is the Kolmogorov constant [36, 37]. Hereafter, this $F_{wc}(z,K)$ is referred to as $F_{neq}(z,K)$. Upon further assuming the inertial subrange scaling extends all the way up to large scales comparable to $\Lambda_c(\zeta)$ without any modification, the conventional scalar-velocity co-spectrum in equation 5 is recovered. Inserting this modeled co-spectrum in equation 9 with $1/(s_c f_{wc} z)$ replacing $1/z$ in the lower integral limit results in

$$\phi_{c\,neq}(\zeta) = \frac{1}{\left(s_c f_{wc}(\zeta)\right)^{4/3}\left(\phi_m(\zeta) - \zeta\right)^{1/3}}. \quad (22)$$

Note that the condition $\phi_c(0) = 1$ eliminates the dependence of $\phi_c(\zeta)$ on constants such as A_π. Hereafter, $\phi_{c\,neq}$ is referred to as the scalar stability correction function for the equilibrium state in the absence of buoyancy forces.

D. The Equilibrium State Modified by Thermal Stratification

If buoyancy effects are allowed to modify the velocity field (i.e., $\beta \neq 0$), the co-spectral budget reduces to

$$0 = \frac{2}{3}\Gamma(z)E(z,K) - A_\pi \frac{F_{wc}(z,K)}{\tau(z,K)} + \frac{4}{3}\beta F_{Tc}(z,K). \quad (23)$$

When the scalar of interest is air temperature, the preceding equation with the definition of $\tau(z,K) = \varepsilon(z)^{-1/3}\ K^{-2/3}$ yields

$$F_{wT}(z,K) = \left[\frac{2\Gamma(z)E(z,K)}{3A_\pi} + \frac{4}{3}\frac{\beta F_{TT}(z,K)}{A_\pi}\right]\frac{K^{-2/3}}{\varepsilon(z)^{1/3}}, \quad (24)$$

where $\Gamma(z)$ is now the mean air temperature gradient. An inertial subrange approximation for $F_{TT}(z,K)$ is employed [38],

$$F_{TT}(z,K) = C_T \varepsilon(z)^{-1/3} N_T(z) K^{-5/3}, \quad (25)$$

where $C_T = 0.8$ is the Kolmogorov-Corrsin constant [38], $N_T(z)$ is the thermal variance dissipation rate and is estimated as $N_T(z) = -\overline{w'T'}\Gamma(z)$ from an equilibrium temperature variance budget equation [18, 39]. Upon employing the equilibrium estimate of $\varepsilon(z)$ in equation 7, equation 24 reduces to

$$F_{wT}(z,K) = \left[1 - \frac{3}{2}\frac{(4/3)C_T}{C_o}\frac{\zeta}{(\phi_m(\zeta) - \zeta)}\right] F_{neq}(z,K). \quad (26)$$

Here also, only the relatively well-known constants C_T and C_o appear, the other constants cancel after imposing $\phi_c(0) = 1$. The factor in squared brackets varies between 0.8 (most stable) and 2.3 (most unstable) and is always positive. It acts to reduce the magnitude of the co-spectrum under stable conditions and to increase it under unstable conditions (as expected). The sign of the co-spectrum is therefore set by the sign of the mean temperature gradient $\Gamma(z)$. Combining this estimate of $F_{wT}(z,K)$ with equation 9, which uses $1/(s_c f_{wc} z)$ to replace $1/z$ as the lower integration limit, we obtain

$$\phi_{T\,eq}(\zeta) = \frac{\phi_{c\,neq}(\zeta)}{\left(1 - \frac{3}{2}\frac{(4/3)C_T}{C_o}\frac{\zeta}{(\phi_m(\zeta)-\zeta)}\right)}. \quad (27)$$

The inclusion of a finite $\beta F_{TT}(z,K)$ can thus significantly modify the temperature stability correction function from its no-buoyancy equilibrium state. Moreover, the outcome is dependent on C_T/C_o not the absolute values of the constants. That is, the outcome here is robust to the precise interpretation of K as being 1-dimensional or 3-dimensional wavenumber. As can be seen from Figure 2, $\phi_{T\,eq}$ follows the measurements closely, at least when compared to $\phi_{T\,neq}$.

E. The Non-Equilibrium State

Upon retaining a finite flux-transport contribution for $K > 1/\Lambda_c$ and invoking inertial subrange approximations for $F_{TT}(z,K)$ as before, the co-spectral budget reduces to

$$\frac{A_4}{K^{2/3}}\frac{\partial}{\partial K}\left(K^{5/3} F_{wT}(z,K)\right) + F_{wT}(z,K) = A_3 K^{-7/3}, \quad (28)$$

where $A_3 = \left[1 - \frac{3}{2}\frac{(4/3)C_T}{C_o}\frac{\zeta}{(\phi_m(\zeta)-\zeta)}\right] C_{wT}\Gamma(z)\varepsilon(z)^{1/3}$ and $A_4 = A_T/A_\pi$; the general solution of this equation is given by

$$F_{wT}(z,K) = \frac{3A_3}{3-2A_4}K^{-7/3} + B_1 K^{-5/3-1/A_4}, \quad (29)$$

where $A_4 \geq 3/2$ [30] and B_1 is an integration constant. When $A_4 = 3/2$, the equation 29 recovers the classical '-7/3' inertial subrange scaling law for $F_{wT}(K)$. When $A_4 = 3$, the leading power-law is an approximate K^{-2} as discussed elsewhere [30, 40]. To evaluate B_1, it is assumed that $\partial F_{wT}/\partial K = 0$ at $K = 1/\Lambda_c$ to ensure a maximum at that peak wavenumber, which results in

$$B_1 = \frac{-(21 A_3 A_4 \Lambda_c^{2/3-1/A_4})}{(9(1+A_4) - 10A_4^2)}. \quad (30)$$

Combining this estimate of B_1 with equations 29 and 9 leads to

$$\phi_T(\zeta) = \phi_T(\zeta)_{eq}\ Y_c(A_4). \quad (31)$$

Hence, contributions originating from the co-spectral flux transport term to eddies whose wavenumber $K > 1/\Lambda_c$ manifest themselves as a multiplier Y_c to $\phi_T(\zeta)$, where $Y_c(A_4) = 4(3+2A_4)(3+5A_4)/(27+81A_4)$ is a constant that varies with A_4. The final equation 31 depends on the value of A_4, again due to its modification of the inertial subrange scaling law of $F_{wT}(K)$. When $A_4 = 3/2$ (corresponding to the '-7/3' power law), $Y_c(A_4) = 1.8$; when $A_4 = 3$ (corresponding to the '-2' power law), $Y_c(A_4) = 2.5$. Nonetheless, these variations in Y_c are not produced by atmospheric stability variations. That is, the addition of a flux transport term affects $\phi_T(\zeta)$ by a multiplier ($= Y_c$) uniformly applied across all atmospheric stability values and as such does not contribute to the variation of $\phi_T(\zeta)$ and Pr with stability, which as discussed in the previous section are rather well-explained by the contribution of the buoyancy term.

III. DISCUSSION

Based on the proposed derivation, the various turbulent processes responsible for the shape of $\phi_T(\zeta)$ in the Kansas experiment can now be unfolded. A logical starting point is the most idealized state – a co-spectral budget reduced to the interplay between mechanical production and dissipation via scalar-pressure interaction known to be far more significant than the molecular terms. The mechanical production requires knowledge of the energy spectrum, which is assumed here to follow inertial subrange scaling, and the dissipation term is modeled via a Rotta type pressure-scalar interaction modified to include buoyancy effects. In this budget, all low-wavenumber contributions to $F_{wc}(z,K)$ (i.e. $K < 1/z$) are either suppressed or assumed to cancel out

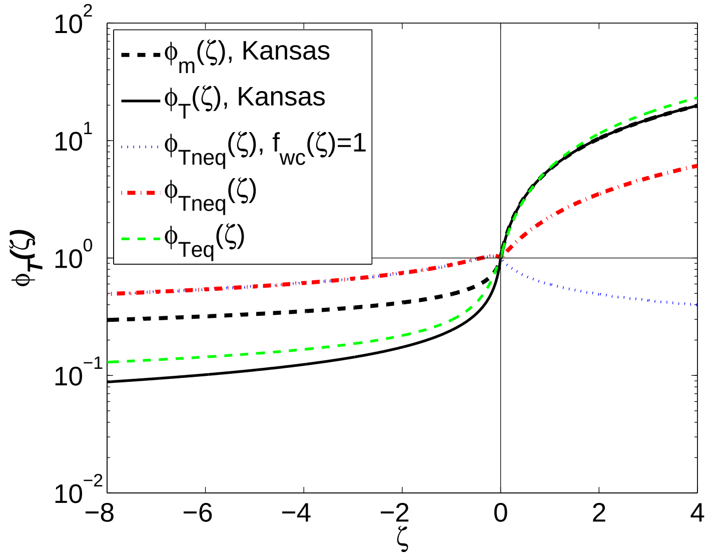

FIG. 2. (Color on-line): The universal shape of $\phi_T(\zeta)$ as determined from the Kansas experiment for heat along with the resulting $\phi_T(\zeta)$ from various approximation to the co-spectral budget F_{wT}, including $\phi_{T_{neq}}(\zeta)$ and $\phi_{T_{eq}}(\zeta)$. The $\phi_{T_{neq}}(\zeta)$ is calculated from equation 22 with $f_{wc}(\zeta) = 1$ so it collapses with $\phi_{T_{neq}}(\zeta)$ when $\zeta < 0$. In the model derivation, inertial subrange scaling is assumed for $E(z,K)$ and $F_{TT}(z,K)$ with no modifications in the low-wavenumber range.

so that $\left|\int_0^{1/z} F_{wc}(z,K)dK\right| \ll \left|\int_{1/z}^{\infty} F_{wc}(z,K)dK\right|$. These approximations to the co-spectral budget result in an $F_{wc}(z,K)$ that follows its conventional inertial subrange shape [22]. Integrating this $F_{wc}(z,K)$ from $K = 1/z$ to ∞ leads to $\phi_{c_{neq}}(\zeta) = \phi_{T_{neq}}(\zeta)$ for any scalar. The resulting behavior from this neutral equilibrium approximation is shown in Figure 2. Comparing this modeled $\phi_{T_{neq}}(\zeta)$ with $f_{wc}(\zeta) = 1$ to the Kansas measured $\phi_T(\zeta)$, it is clear that this model cannot reproduce many features of the Kansas (and many other) experiments such as the increases in measured $\phi_T(\zeta)$ for $\zeta > 0$. For $\zeta < 0$, the modeled $\phi_{T_{neq}}(\zeta)$ decays with increasing $-\zeta$ but its value remains much larger than the measured $\phi_T(\zeta)$, or for that matter, $\phi_m(\zeta)$. Revising the lower integration limit of the modeled co-spectrum to $K = 1/\Lambda_c$ instead of $1/z$ to obtain $\phi_{T_{neq}}(\zeta)$ leads to an increase with increasing ζ for stable conditions, though not at the same rate as those reported for the Kansas experiment. Hence, the dependence of Λ_c on ζ has some effect on $\phi_T(\zeta)$ for stable conditions, but this effect is not sufficient to reproduce the rapid increase in $\phi_T(\zeta)$ when $\zeta > 0$. In short, a balance between production and dissipation with $E(z,K)$ following its inertial subrange laws alone and without any buoyancy contribution (i.e. without a finite β) cannot reproduce the Kansas reported $\phi_T(\zeta)$.

Adding the buoyancy term and assuming that the temperature spectrum also follows its inertial subrange shape from $K = 1/\Lambda_c$ to ∞, the agreement between measured

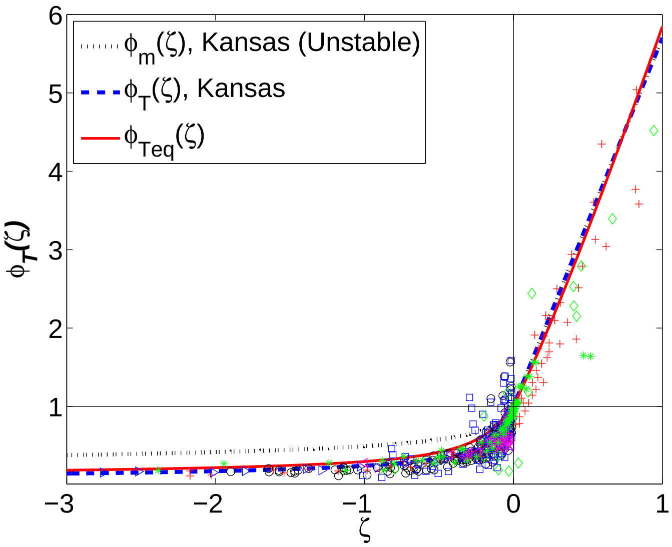

FIG. 3. (Color on-line): Comparison between measured $\phi_T(\zeta)$ for the data sources in Figure 1 and modeled $\phi_{T_{eq}}(\zeta)$ from the full co-spectral budget. Note the large scatter in the data for $-\zeta \to 0$.

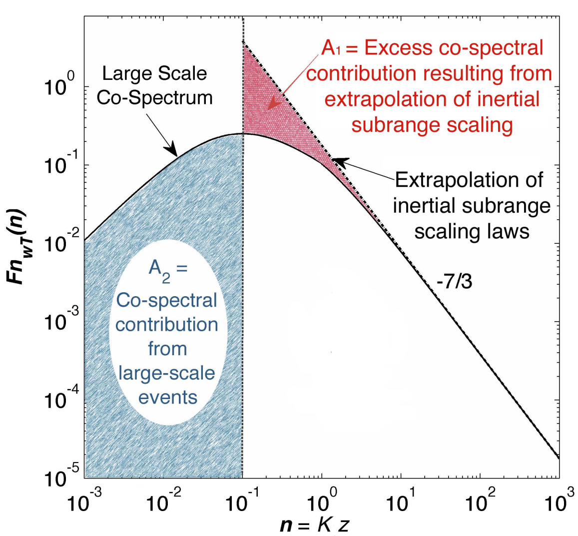

FIG. 4. (Color on-line): The canonical shape of normalized $F_{wT}(z, K)$ as reported in the Kansas experiment against the normalized wavenumber (n) showing a peak at $K = 1/\Lambda_c$, and a $-7/3$ scaling for $K \gg 1/\Lambda_c$ in the inertial subrange. The cumulative contribution of eddies whose $K < 1/\Lambda_c$ is some 50% of the total heat flux (i.e. A_2 is some 50% of the total area under the co-spectrum; note that the areas under the curves are not visually equal due to the double-logarithmic representation). In the derivation leading to $\phi_{T_{eq}}(\zeta)$, neglecting their integrated contribution was partially compensated for by inertial subrange extrapolations of modeled $F_{wT}(K)$ up to $K = 1/\Lambda_c$, indicated by A_1.

and modeled $\phi_{T_{eq}}(\zeta)$ is now significantly improved for unstable conditions. Likewise, for stable conditions, the agreement is greatly improved when the constant α is set to 1.7 in the $f_{wc}(\zeta)$ formulation. It should be emphasized here that the linear dependence of $f_{wc}(\zeta)$ on ζ for stable conditions was reported in the Kansas experiment and was derived independently from the stability correction functions. Thus, it is justifiable to include $f_{wc}(\zeta)$ dependence on ζ for stable conditions independent from the inclusion of the buoyancy term in the conservation equation. However, this value of α is lower than the reported value from the Kansas experiment by a factor commensurate with the 'excess' flux attributed to the difference between modeled and measured $\left|\int_{1/\Lambda_c}^{\infty} F_{wc}(K)dK\right|$. Specifically, the excess flux in the model primarily originates from a flattening in the Kansas measured $F_{wc}(K)$ as $K = 1/\Lambda_c$ is approached while modeled $F_{wc}(K)$ maintains its inertial subrange scaling up to $K = 1/\Lambda_c$ as illustrated in Figure 4. Not withstanding this modification to α, the temperature spectrum remains necessary for recovering $\phi_T(\zeta)$ from the Kansas experiment and for explaining why $Pr < 1$ for unstable conditions as evidenced by Figure 1. This confirms the hypothesized links in previous studies between the active role of temperature and the decrease in Pr under unstable conditions [41, 42]. Li et al. [42] related the dissimilarity between momentum and heat transfer under unstable conditions to a decrease in the ratio of the integral length scale of temperature fluctuations and vertical velocity from roughly 10 to unity with increasing $-\zeta$. At that point, it was argued that the 'resonance' between these two scales becomes important. Upon replacing the temperature with the longitudinal velocity time series, the integral length scale ratio did not approach unity with increasing $-\zeta$. Their conclusion is in broad agreement with the role of buoyancy uncovered here.

When the co-spectral flux transport term is also introduced via a first-order closure model in the spectral domain, the agreement is not dramatically altered except via a constant multiplier that also leads to $\phi_T(0)$ no longer unity. To what degree the experiments can discern a $\phi_T(0) \neq 1$ can be debated. For near-neutral conditions (i.e. $\zeta \to 0$), the scatter in the $\phi_T(\zeta)$ measurements is not small as shown in Figure 3 presumably due to the small sensible heat flux $(= \overline{w'T'})$ and a small mean air temperature gradient (i.e. Γ). A small heat flux accompanied by a small mean air temperature gradient produces large uncertainties in measured $\phi_T(0)$ as evidenced by the definition in equation 4.

Departures in $\phi_T(\zeta)$ from the Kansas experiment have been reported and reviewed elsewhere [11]. A common explanation in all these experiments is the role of large eddies. In fact, using the Kansas reported $F_{wT}(K)$ for unstable conditions leads to $\left|\int_0^{1/\Lambda_c} F_{wT}(K)dK\right| \approx$

$\left| \int_{1/\Lambda_c}^{\infty} F_{wT}(K) dK \right|$. That is, eddies larger than Λ_c contribute some 50% of the total scalar flux (for unstable conditions) based on Kansas measured $F_{wc}(K)$ and can thus have significant impact on $\phi_T(\zeta)$. Neglecting their contribution in the derivation leading to $\phi_{T_{eq}}(\zeta)$ here was partially compensated for by the inertial subrange extrapolation of modeled $F_{wT}(K)$ up to $K = 1/\Lambda_c$ as shown in Figure 4. To what degree this compensation is complete and to what degree the dynamics of the fluxes contributed by these larger scale eddies are universal remains debatable and explain why several experiments report large fluctuations, or even anomalous scaling, in $\phi_T(\zeta)$. The generation and the impinging mechanisms of large eddies onto the atmopsheric surface layer are diverse and vary with atmospheric stability. For experiments in which the terrain was flat and the surface cover was uniform, these mechanisms may include detached eddies generated by shearing motions in the neutral boundary layer, convective motion in the outer layer of the convective boundary layer, and attached eddies initiated by instabilities within the atmopsheric surface layer [8, 43–45]. Even for neutral conditions, laboratory studies have also documented the impingement of large (and very large) structures onto the 'logarithmic' region at high Reynolds number [46–48]. Clearly, these large-scale processes cause non-universal departure from inertial subrange scaling in both $E(K)$ and $F_{TT}(K)$, and introduce low-frequency modulations in $F_{wT}(K)$ that must be included. If known, these inertial subrange departures and low frequency modulations can be accommodated in this co-spectral framework on a case-by-case basis.

On the topic of large scales modulations, it would be a remiss if we did not recall a statement made by Lumley and Yaglom [49] who noted that *Julian Hunt now claims (private communication) that these* (i.e. the Kansas) *data are seriously filtered at low wavenumbers. There are evidently data of Högström at Uppsala that were suppressed for decades because they did not agree with the Kansas data at low wavenumber, which suggest the presence of elongated coherent structures*. The Högström data were collected under conditions of much worse terrain inhomogeneity than in Kansas, and it is conceivable that the idealized atmospheric surface layer assumptions (e.g. stationary, planar-homogeneous assumption lacking subsidence or mean longitudinal pressure gradients) necessary for the application of MOST were not fully satisfied. Hence, the final clarification of how low-wavenumber contributions modify $\phi_T(\zeta)$ in the Kansas (and Uppsala) experiments must be left to the future, where further sensitivity to different non-stationary trend removal techniques can be fully explored. Nonetheless, when all these results are taken together, it appears that the 'universal' features in $\phi_T(\zeta)$ can be attributed to processes tightly linked to those leading to the derivation of $\phi_{T_{eq}}(\zeta)$, which inherit their 'universal' character from well-established inertial subrange scaling laws. This is also in agreement with Gioia et al. [50], who concluded that the log-layer in their neutral cases results from inertial subrange eddies and scaling.

IV. CONCLUSION

The extensive measurements made in Kansas by Kaimal and Wyngaard has served as benchmarks in atmospheric surface layer flows for decades. It was shown here that the universal shape of $\phi_T(\zeta)$ reported from these experiments is remarkably consistent with inertial subrange theories describing the velocity and temperature spectra using a simplified co-spectral budget across a wide range of ζ. Moreover, it was shown that the contributing role to $\phi_T(\zeta)$ by buoyancy (via the temperature spectrum) is the leading order explanation for the anomalous departure from Reynolds analogy. Hence, the long-surmised link between the energetics of the micro-state of turbulence (encoded in the temperature and energy spectra) and the macro-state property of the bulk flow (encoded here in $\phi_T(\zeta)$) was explicitly revealed. As was recently accomplished in linking the mean velocity profile and the spectrum of turbulence by Gioia et al. [50], the co-spectral link derived here establishes a blue-print for a framework to assess how large-scale structures impinging on the atmospheric surface layer may modify $\phi_T(\zeta)$, and can perhaps lead to improved representation of the mass exchange rates in future large-scale models.

ACKNOWLEDGMENTS

GK is partly supported by the U.S. Department of Energy through the Office of Biological and Environmental Research (BER) Terrestrial Carbon Processes (TCP) program (DE-SC000697), the U.S. National Science Foundation (NSF) under NSF-EAR-10-13339 and NSF-AGS-1102227, and the U.S. Department of Agriculture (2011-67003-30222). EBZ and DL are supported by NSF under AGS-1026636 and CBET-1058027, and MC is supported by NSF under AGS-0638385.

[1] A. Monin and A. Obukhov, Akad. Nauk. SSSR. Geofiz. Inst. Trudy **151**, 163 (1954).
[2] A. Monin and A. M. Yaglom, *Statistical Fluid Mechanics*, Vol. 1 (MIT Press, Cambridge, 1971).
[3] T. Foken, Boundary Layer Meteorology **119**, 431 (2006).
[4] J. A. Businger, J. C. Wyngaard, Y. Izumi, and E. F. Bradley, Journal of the Atmospheric Science **28**, 181 (1971).

[5] W. Brutsaert, *Evaporation into the atmosphere: Theory, history, and applications*, Environmental Fluid Mechanics (Kluwer Academic Publishers, Dordrecht, 1982).
[6] O. Moraes, Boundary Layer Meteorology **96**, 317 (2000).
[7] B. A. Kader and A. M. Yaglom, Journal of Fluid Mechanics **212**, 637 (1990).
[8] A. Smedman, U. Högström, J. Hunt, and E. Sahlee, Quarterly Journal of the Royal Meteorological Society **133**, 37 (2007).
[9] W. O. Pruitt, D. L. Morgan, and F. Lourence, Quarterly Journal of the Royal Meteorological Society **99**, 370 (1973).
[10] K. Schmitt, C. Friehe, and C. Gibson, Journal of the Atmospheric Sciences **36**, 602 (1979).
[11] Y. Zhang, H. Liu, T. Foken, Q. Williams, S. Liu, M. Mauder, and C. Liebethal, Boundary Layer Meteorology **136**, 235 (2010).
[12] A. Obukhov, Trudy Inta Teoret. Geofiz. Akad. Nauk. S.S.S.R. , 95 (1946).
[13] J. A. Businger and A. M. Yaglom, Boundary Layer Meteorology **2**, 3 (1971).
[14] J. Wyngaard and O. Cote, Quarterly Journal of the Royal Meteorological Society **98**, 590 (1972).
[15] J. Kaimal and J. Finnigan, *Atmospheric boundary layer flows: Their structure and measurement* (Oxford University Press, New York, 1994).
[16] G. Taylor, Proceedings of the Royal Society of London A **132**, 476 (1938).
[17] U. Frisch, *Turbulence* (Cambridge University Press, Cambridge, England, 1995).
[18] H. Tennekes and J. Lumley, *A first course in turbulence* (MIT Press, Cambridge, 1972).
[19] J. Lumley, Physics of Fluids **10**, 855 (1967).
[20] S. Saddoughi and S. Veeravalli, Journal of Fluid Mechanics **268**, 333 (1994).
[21] R. Fleagle and J. Businger, *An introduction to atmospheric physics* (Academic Press, New York, 1963).
[22] J. Lumley and H. Panofsky, *The structure of atmospheric turbulence* (John Wiley and Sons, New York, 1964).
[23] J. Businger, Boundary Layer Meteorology **42**, 145 (1988).
[24] S. Khanna and J. G. Brasseur, Journal of Fluid Mechanics **345**, 251 (1997).
[25] A. J. Dyer and B. B. Hicks, Quarterly Journal of the Royal Meteorological Society **96**, 715 (1970).
[26] A. J. Dyer, Boundary-Layer Meteorology **7**, 363 (1974).
[27] H. de Bruin, Journal of Applied Meteorology **38**, 626 (1999).
[28] G.G. Katul, A.G. Konings, and A. Porporato, Physical Review Letters **107**, 268502 (2011).
[29] A. A. Townsend, *The structure of turbulent shear flow*, Vol. 2 (Cambridge University Press, Cambridge, 1976).
[30] W. Bos, H. Touil, L. Shao, and J. Bertoglio, Physics of Fluids **16**, 3818 (2004).
[31] W. Bos and J. Bertoglio, Physics of Fluids **19**, 025104 (2007).
[32] J. Deardorff, Workshop on Micrometeorology, American Meteorological Society, Ed. Haugen, D.A. **Boston**, 271 (1973).
[33] J. Andre, G. De Moor, P. Lacarrere, G. Therry, and R. du Vachat, Turbulent Shear Flows **1**, 307 (1979).
[34] C. Moeng and J. Wyngaard, Journal of the Atmospheric Sciences **43**, 2499 (1986).
[35] K. Choi and J. Lumley, Journal of Fluid Mechanics **436**, 59 (2001).
[36] A. Kolmogorov, Dokl Akad. Nauk. SSSR **30**, 9 (1941).
[37] P. K. Yeung and Y. Zhou, Physical Review E **56**, 1746 (1997).
[38] S. Corrsin, Journal of Applied Physics **22**, 469 (1951).
[39] C. Hsieh and G. Katul, Journal of Geophysical Research **102**, 16391 (1997).
[40] D. Cava and G. Katul, Boundary Layer Meteorology **To appear** (2012).
[41] D. Li and E. Bou-Zeid, Boundary-Layer Meteorology **140**, 243 (2011).
[42] D. Li, G. Katul, and E. Bou-Zeid, Physics of Fluids , 105105.
[43] J. C. Kaimal, J. C. Wyngaard, D. A. Haugen, O. R. Cote, Y. Izumi, S. J. Caughey, and C. J. Readings, Journal of the Atmospheric Sciences **33**, 2152 (1976).
[44] K. McNaughton and Y. Brunet, Boundary Layer Meteorology **102**, 161 (2002).
[45] K. McNaughton, R. Clement, and J. Moncrieff, Nonlinear Processes in Geophysics **14**, 257 (2007).
[46] I. Marusic, B. McKeon, P. Monkewitz, H. Nagib, A. Smits, and K. Sreenivasan, Physics of Fluids **22**, 1 (2010).
[47] I. Marusic, R. Mathis, and N. Hutchins, Science **329**, 193 (2010).
[48] A. Smits, B. McKeon, and I. Marusic, Annual Review of Fluid Mechanics **43**, 353 (2011).
[49] J. Lumley and A. Yaglom, Flow, Turbulence and Combustion **66** (2001).
[50] G. Gioia, N. Guttenberg, N. Goldenfeld, and P. Chakraborty, Physical Review Letters **105**, 184501 (2010).